An improved tetracycline-inducible expression system for fission yeast

Xiao-Hui Lyu[1], Yu-Sheng Yang[1], Zhao-Qian Pan[1], Shao-Kai Ning[1], Fang Suo[1], Li-Lin Du[1,2]

[1]National Institute of Biological Sciences, Beijing 102206, China

[2]Tsinghua Institute of Multidisciplinary Biomedical Research, Tsinghua University, Beijing 102206, China

*Corresponding author: dulilin@nibs.ac.cn (L.-L.D.)

Running head: Inducible system for *S. pombe*.

Keywords: inducible expression system, fission yeast, *Schizosaccharomyces pombe*, tetracycline, conditional loss-of-function

Abstract

The ability to manipulate gene expression is valuable for elucidating gene function. In the fission yeast *Schizosaccharomyces pombe*, the most widely used regulatable expression system is the *nmt1* promoter and its two attenuated variants. However, these promoters have limitations, including a long lag, incompatibility with rich media, and unsuitability for non-dividing cells. Here, we present a tetracycline-inducible system free of these shortcomings. Our system features the *enotetS* promoter, which achieves a similar induced level and a higher induction ratio compared to the *nmt1* promoter, without exhibiting a lag. Additionally, our system includes four weakened *enotetS* variants, offering an expression range similar to the *nmt1* series promoters but with more intermediate levels. To enhance usability, each promoter is combined with a Tet-repressor-expressing cassette in an integration plasmid. Importantly, our system can be used in non-dividing cells, enabling the development of a synchronous meiosis induction method with high spore viability. Moreover, our system allows for the shutdown of gene expression and the generation of conditional loss-of-function mutants. This system provides a versatile and powerful tool for manipulating gene expression in fission yeast.

Introduction

Understanding gene function is a central pursuit in biological studies. One important approach to dissecting the function of individual genes is through the artificial manipulation of gene expression levels. Over the past 35 years, a large number of regulatable promoter systems have been developed to enable the manipulation of gene expression in the fission yeast *Schizosaccharomyces pombe*. These systems include glucose-repressible promoters (Hoffman and Winston, 1989; Iacovoni et al., 1999), hormone-inducible promoters (Ohira et al., 2017; Picard et al., 1990), thiamine-repressible promoters and their derivatives (Basi et al., 1993; Garg, 2020; Kjaerulff and Nielsen, 2015; Kumar and Singh, 2006; Maundrell, 1993, 1990; Moreno et al., 2000), tetracycline-inducible promoters (Erler et al., 2006; Faryar and Gatz, 1992; Patterson et al., 2019; Zilio et al., 2012), a copper-repressible promoter (Bellemare et al., 2001), a heat shock-inducible promoter (Fujita et al., 2006), a uracil-inducible promoter (Watson et al., 2011; Watt et al., 2008), an ethanol-inducible promoter (Matsuzawa et al., 2013), and pheromone-inducible promoters (Hennig et al., 2018).

Among the various regulatable promoters available for *S. pombe*, the most popular ones are three thiamine-repressible promoters based on that of the *nmt1* gene (Basi et al., 1993; Maundrell, 1993, 1990). This promoter system offers several advantages. Firstly, the *nmt1* promoter (*Pnmt1*) is a highly active promoter when induced, as *nmt1* ranks as the eighth most highly transcribed protein-coding gene in vegetative cells (340 mRNA molecules per cell) (Marguerat et al., 2012). Secondly, there are two weakened promoter variants, *P41nmt1* and *P81nmt1*, which allow for lower levels of expression, approximately one and two orders of magnitude lower than *Pnmt1*, respectively (Basi et al., 1993). Thirdly, these promoters are strongly repressed in the presence of thiamine, resulting in an around 100-fold difference in expression level between the induced and repressed states (Basi et al., 1993; Vještica et al., 2020). However, this system is not without limitations. It is not compatible with yeast extract-

55 based rich media that contain thiamine. Additionally, induction requires a medium switch,
56 which incurs time and labor costs. The most significant drawback is that the intracellular
57 thiamine concentration needs to be diluted through several cell doublings before induced
58 expression can occur (Maundrell, 1990; Tommasino and Maundrell, 1991). This results in a
59 long lag time of around 10-12 h and makes the system unsuitable for non-dividing cells such
60 as cells in a quiescent state.

61 Tetracycline-inducible systems based on the Tet repressor-operator system of the
62 bacterial transposon Tn*10* have been widely used to manipulate gene expression in
63 eukaryotes (Berens and Hillen, 2003; Hillen et al., 1984, 1983). A basic version of the
64 tetracycline-inducible systems consists of three components: the *tet* operator DNA sequence
65 (*tetO*), which is incorporated into a promoter; the Tet repressor protein (TetR), which has a
66 high binding affinity to *tetO*; and a small-molecule inducer that prevents TetR from binding to
67 *tetO*. Commonly used inducers include tetracycline and its analogs anhydrotetracycline
68 (ahTet) and doxycycline. In the absence of the inducer, TetR binds to *tetO* and represses the
69 transcription of the downstream gene. When the inducer is added, TetR no longer binds to
70 *tetO*, and the transcription of the downstream gene is induced.

71 Three different tetracycline-inducible promoters have been used in fission yeast. In 1992,
72 Faryar and Gatz established the first tetracycline-inducible promoter for fission yeast by
73 incorporating three *tetO* sequences into the cauliflower mosaic virus 35S (CaMV35S)
74 promoter (Faryar and Gatz, 1992). This tetracycline-inducible promoter can be quickly
75 induced, with the expression product becoming detectable within two hours after the addition
76 of an inducer (Faryar and Gatz, 1992). However, an independent study showed that this
77 system has an induction ratio of only 10-fold and the induced expression level is low, similar
78 to that of *P81nmt1* (Forsburg, 1993). In 2012, Zilio et al. adapted a tetracycline-inducible
79 system, originally developed for the budding yeast *Saccharomyces cerevisiae*, for use in the

80 fission yeast (Bellí et al., 1998; Garí et al., 1997; Zilio et al., 2012). The promoter in this
81 system is composed of seven *tetO* sequences and the basal promoter of the budding yeast
82 *CYC1* gene. The induced level of expression of this promoter is also low, similar to that of
83 *P81nmt1* (Zilio et al., 2012). In 2019, a much stronger tetracycline-inducible promoter, called
84 the *enoTet* promoter (*PenoTet*), was developed by placing three *tetO* sequences into the
85 promoter of the *S. pombe eno101* gene (Patterson et al., 2019). The *eno101* gene is the
86 fourth most highly transcribed protein-coding gene in vegetative cells (470 mRNA molecules
87 per cell) (Marguerat et al., 2012). *PenoTet* achieves an induced expression level about 50%
88 as high as that of *Pnmt1* (Patterson et al., 2019). Unlike the *nmt1* series promoters, these
89 tetracycline-inducible promoters are compatible with rich media, do not need a medium
90 switch for induction, do not exhibit an obvious lag time, and can be used in non-dividing cells.
91 However, these promoters have not been widely adopted, potentially due to the lack of multi-
92 level options, insufficient induced expression levels, non-ideal induction ratios, and the
93 inconvenience associated with the need to introduce both a tetracycline-inducible promoter
94 and a TetR-expressing cassette into a host strain.

95 In the present study, we have developed an improved tetracycline-inducible expression
96 system for *S. pombe*. This system includes a strong promoter, *PenotetS*, which, similar to
97 *PenoTet*, is derived from the *eno101* promoter but contains only a single *tetO* sequence.
98 *PenotetS* has a high induction ratio of approximately 200-fold and its induced level is similar
99 to that of *Pnmt1*. Additionally, our system includes four weakened variants of *PenotetS*,
100 allowing for five different levels of induced expression. For ease of use, a collection of
101 integration plasmids was constructed, each containing an *enotetS* series promoter and a
102 TetR-expressing cassette. Capitalizing on the compatibility of this system with non-dividing
103 cells, we have developed a new method to induce meiosis, resulting in favorable spore
104 viability and synchrony. Moreover, we have successfully employed this system to generate

105 conditional lethal mutants of essential genes, underscoring its versatility and applicability.

Results

The development of a strong inducible promoter *PenotetS*

It has been shown that in the case of the *GAL1* promoter of *Saccharomyces cerevisiae*, placing a single *tetO* sequence between the TATA box and the transcription start site (TSS) is sufficient to render the promoter strongly repressible by TetR (Murphy et al., 2007). We adopted this approach to modify the 276-bp promoter of the *S. pombe eno101* gene (Wang et al., 2014), which was the basis of the *PenoTet* promoter that contains three *tetO* sequences (Patterson et al., 2019). In *S. pombe* promoters, the TATA box and the TSS, each possessing distinct sequence characteristics, are typically separated by a constant distance (Li et al., 2015; Lu and Lin, 2021; Russell, 1983; Thodberg et al., 2019). To maintain this distance, we substituted a 19-bp sequence between the TATA box and the TSS of the *eno101* promoter with a 19-bp *tetO* sequence (Fig. 1A). We named the modified promoter *PenotetS*, with the letter "*S*" indicating the presence of a single copy of the *tetO* sequence.

A drawback of some of the previously published tetracycline-inducible systems for *S. pombe* is the inconvenience caused by the need to separately introduce a tetracycline-inducible promoter and a TetR-expressing cassette. To establish a user-friendly system, we combined *PenotetS* with a TetR-expressing cassette, which consists of the cytomegalovirus (CMV) promoter and the TetR coding sequence, in a stable integration vector (SIV) (Vještica et al., 2020) (Fig. 1B). The CMV promoter is a robust constitutive promoter in *S. pombe* (Amelina et al., 2016; Toyama and Okayama, 1990). Additionally, downstream of *PenotetS*, we inserted the coding sequence for the yellow fluorescent protein mECitrine, followed by the terminator sequence derived from the *ADH1* gene of *Saccharomyces cerevisiae*. The resulting plasmid was named pDB5318. The fluorescence emitted by mECitrine serves as an indicator of the expression level of *PenotetS*.

In *S. pombe*, previous studies have shown that anhydrotetracycline (ahTet), an analog

131 of tetracycline, is a more effective inducer compared to tetracycline and doxycycline (Erler et
132 al., 2006; Zilio et al., 2012). When an *S. pombe* strain containing pDB5318 was cultured in
133 YES medium supplemented with 2.5 μg/ml of ahTet, a concentration used in a previous study
134 (Zilio et al., 2012), it was observed that the expression level of *PenotetS* was higher than that
135 of the strong constitutive promoter *Padh1* (Fig. 1D). In the absence of ahTet, the expression
136 level of *PenotetS* was markedly lower than that of *Padh1*. Thus, *PenotetS* is an inducible
137 promoter with a high level of induced expression and a substantial induction ratio.
138
139 **The development of four weakened variants of *PenotetS***
140 To provide a range of different expression levels, we developed four weakened variants of
141 *PenotetS*. The design was inspired by a previous study that used GC-rich stem-loop-forming
142 sequences inserted in the 5′ UTR to reduce gene expression (Lamping et al., 2013). It was
143 shown that the extent of expression attenuation increases with the number of GC base pairs
144 in the stem. We selected four different stem-loop-forming sequences used in that study (Fig.
145 1C). Each sequence was inserted immediately downstream of *PenotetS*. The resulting
146 promoters were named *PenotetSW1*, *PenotetSW2*, *PenotetSW3*, and *PenotetSW4*. The
147 letter "W" indicates a weakened variant, while the number denotes the expected expression
148 strength, with *PenotetSW1* being the highest and *PenotetSW4* being the lowest.
149 These weakened promoters were combined with the TetR-expressing cassette in an SIV
150 plasmid, following the same procedure as *PenotetS*. In YES medium supplemented with 2.5
151 μg/ml of ahTet, the expression strengths of these promoters varied as expected (Fig. 1D).
152 *PenotetSW1* exhibited an expression level similar to that of *Padh1*, while the other three
153 promoters showed progressively lower levels. In the absence of ahTet, the expression level
154 of each promoter was dramatically lower compared to when ahTet was present, with the
155 three weaker promoters showing fluorescence signals that were indistinguishable from the

156 background.

157

158 **Inducer dose response**

159 We assessed the inducer dose response of *PenotetS* in both YES and EMM media. The
160 inducer ahTet was used at various concentrations, ranging from 0.004 μg/ml to 2.5 μg/ml.
161 After a 24-hour induction period (which was long enough to reach a steady-state level; see
162 below), the expression levels were measured using the fluorescence signal of the reporter
163 protein mECitrine (Fig. 2). In both types of media, a dramatic transition from a near-minimal
164 level to a near-maximal level was observed between two doses that differed by 5-fold. In
165 YES, this transition occurred between 0.004 μg/ml and 0.02 μg/ml of ahTet, while in EMM, it
166 occurred between 0.02 μg/ml and 0.1 μg/ml of ahTet. Similar steep dose-response patterns
167 have been observed in other published eukaryotic tetracycline-inducible systems that utilize
168 constitutively expressed TetR as a repressor (Azizoglu et al., 2021; Erler et al., 2006;
169 Nevozhay et al., 2009). We chose to use 2.5 μg/ml of ahTet, an inducer concentration well
170 above the saturating level in both types of media, for subsequent experiments.

171

172 **Induction kinetics in dividing cells**

173 We next assessed the induction kinetics of *PenotetS* and *PenotetSW2* by performing
174 induction time course experiments in both YES and EMM media (Fig. 3). In all time courses,
175 the expression level of the reporter protein mECitrine increased by more than two orders of
176 magnitude within the first 10 hours following the addition of ahTet and ceased to increase
177 after 12 hours. We used the expression level at the 24-hour time point as the steady-state
178 level. In YES medium, for both promoters, at the one-hour time point after adding ahTet to
179 the cultures, the fluorescence signal of mECitrine had already increased by more than one
180 order of magnitude, reaching around 10% of the steady-state level. This rapid increase

181 suggests that both promoters were turned on quickly after the addition of ahTet. In EMM
182 medium, the initial phase of the induction was slightly slower, reaching around 5% of the
183 steady-state level at the one-hour time point. In both types of media, at the four-hour time
184 point, both promoters had reached or surpassed 50% of the steady-state level. By the eight-
185 hour time point, both promoters had reached within 15% of the steady-state level.

186 Upon the activation of an inducible promoter that drives the expression of a protein-
187 coding gene, the level of the protein product reaches a steady state when its synthesis is
188 balanced by its degradation and dilution (Azizoglu et al., 2021; Rosenfeld et al., 2002). The
189 steady-state expression level is determined by both the synthesis rate and the degradation-
190 and-dilution rate, while the induction kinetics are solely determined by the degradation-and-
191 dilution rate (Rosenfeld et al., 2002). Fluorescent proteins are highly stable and have in vivo
192 half-lives longer than 20 hours (Corish and Tyler-Smith, 1999; He et al., 2019; Perruca-
193 Foncillas et al., 2022). In our experimental setup, given that the doubling time of proliferating
194 *S. pombe* cells is around 3 hours (Petersen and Russell, 2016), the degradation-and-dilution
195 rate of mECitrine should mainly be determined by its dilution through cell division. In this
196 scenario, without considering any delay between transcription activation and the formation
197 of mECitrine protein capable of emitting fluorescence, the time required to reach 50% of the
198 steady-state expression level theoretically equals the doubling time (Rosenfeld et al., 2002).
199 However, nascent fluorescent proteins only become fluorescent after undergoing a
200 maturation process, which takes approximately 30 minutes for mECitrine (Azizoglu et al.,
201 2021). Taking this delay into account, the induction kinetics observed in our experiments align
202 closely with immediate or near-immediate transcription activation upon the addition of ahTet.
203

204 **Quantification of expression levels and comparison with the *nmt1* series promoters**

205 Next, we conducted a comprehensive quantitative analysis of the induced and repressed

206 expression levels of all *enotetS* series promoters in YES and EMM media, and made
207 comparisons with *Padh1* in YES medium and the *nmt1* series promoters in EMM medium
208 (Fig. 4). In YES medium, the induced expression level of *PenotetS* was approximately 1.6-
209 fold that of *Padh1* (Fig. 4A). The fold differences between the induced level of *PenotetS* and
210 the induced levels of the four weakened *enotetS* series promoters were approximately 1.7-
211 fold, 7.1-fold, 30-fold, and 53-fold, respectively (Fig. 4A). The fold differences between the
212 induced and repressed levels (induction ratios) were about 230-fold for both *PenotetS* and
213 *PenotetSW1* (Fig. 4A). Since the repressed levels of *PenotetSW2*, *PenotetSW3*, and
214 *PenotetSW4* were very close to the background, we could only determine that these levels
215 were below a threshold (THR) for accurate measurement (Fig. 4A).

216 In EMM medium, the induced and repressed expression levels of the *enotetS* series
217 promoters mirrored those observed in YES medium (Fig. 4B, C). When compared to the *nmt1*
218 series promoters, the induced expression level of *PenotetS* was the same as *Pnmt1* and the
219 induced levels of *PenotetSW2* and *PenotetSW4* were similar to those of *Pnmt41* and
220 *P81nmt1*, respectively (Fig. 4B, C). Therefore, in comparison to the *nmt1* series promoters,
221 the *enotetS* series promoters span the same range of induced levels but provide more
222 intermediate levels. Using the mRNA level of the *nmt1* gene in vegetative cells (340 mRNA
223 molecules per cell) as a reference (Marguerat et al., 2012; Rutherford et al., 2024), the
224 induced expression levels of *PenotetS*, *PenotetSW1*, *PenotetSW2*, *PenotetSW3*, and
225 *PenotetSW4* correspond to approximately 340, 200, 48, 11, and 6 mRNA molecules per cell,
226 respectively. Regarding repressed expression levels, the *enotetS* series promoters had lower
227 repressed levels than the *nmt1* series promoters when comparing promoters with similar
228 induced levels. In our experiments, *Pnmt1* exhibited only a 25-fold induction ratio, which is
229 lower than the reported induction ratio of around 100-fold (Basi et al., 1993; Vještica et al.,
230 2020). The reason behind this discrepancy is unclear. Nevertheless, even when considering

231 the reported induction ratio for comparison, the *enotetS* series promoters still outperformed
232 the *nmt1* series promoters in this aspect.
233
234 **Induction kinetics and expression levels in quiescent cells**
235 One limitation of the *nmt1* series promoters is their unsuitability for non-dividing cells, as the
236 induction of these promoters requires the dilution of intracellular thiamine through multiple
237 rounds of cell division after shifting the cells to a thiamine-free medium. Tetracycline-inducible
238 systems should be free of this limitation. Therefore, we tested whether *PenotetS* can function
239 in two types of non-dividing cells: cells arrested in the G0 cell cycle phase through nitrogen
240 starvation and spores (Fig. 5).
241 The basal expression levels of *PenotetS* in G0 cells and spores, as reported by the
242 fluorescence of mECitrine, were slightly higher than the basal level in the dividing cells (Fig.
243 5C), presumably due to the lack of dilution of mECitrine through cell division. Upon the
244 addition of ahTet to G0 cells and spores, the expression of mECitrine from *PenotetS*
245 increased several-fold within the first hour and reached a level similar to the steady-state
246 level in the dividing cells at the eight-hour time point. Unlike the situation in the dividing cells,
247 where the expression of mECitrine from *PenotetS* reached a steady state at the 12-hour time
248 point, the level of mECitrine continued to increase in G0 cells and spores after the 12-hour
249 time point (Fig. 5C). The increase did not stop after the 24-hour time point and the level of
250 mECitrine reached several-fold higher than the steady-state level in the dividing cells at the
251 36-hour time point (Fig. 5C). The prolonged rise time and the higher induced levels in G0
252 cells and spores can be explained by the degradation-and-dilution rate of mECitrine no longer
253 being determined by its dilution through cell division but rather by the degradation of
254 mECitrine, which has a long half-life. A reduced degradation-and-dilution rate of mECitrine
255 leads to a higher steady-state level and an increase in the time required to reach 50% of the

256 steady-state expression level (Rosenfeld et al., 2002).

257

258 **Meiosis induction in *h+/h+* diploids using *PenotetSW1*-expressed Mc-2A-Mi**

259 In *S. pombe,* the most commonly used method to induce synchronous meiosis is through the
260 inactivation of a negative regulator of meiosis, Pat1, using a temperature-sensitive allele of
261 the *pat1* gene, *pat1-114*, in diploid cells homozygous for the mating type (*h+/h+* or *h−/h−*)
262 (Bähler et al., 1991; Iino and Yamamoto, 1985). However, this approach has several
263 drawbacks, including the use of non-physiological temperature and low spore viability (Bähler
264 et al., 1991; Chikashige et al., 2004; Cipak et al., 2012; Guerra-Moreno et al., 2012;
265 Yamamoto and Hiraoka, 2003). The development of ATP analog-sensitive alleles of *pat1* has
266 enabled the induction of synchronous meiosis at physiological temperature (Cipak et al.,
267 2012; Guerra-Moreno et al., 2012). Moreover, combining Pat1 inactivation with the
268 expression of the *matP*-cassette-encoded protein Pc in *h−/h−* diploids has been shown to
269 elevate spore viability to near-wild-type levels (Cipak et al., 2012; Yamamoto and Hiraoka,
270 2003). Thus, the current state-of-the-art approach for achieving synchronous meiosis with
271 normal spore viability in *S. pombe* requires the combination of two genetic modifications. To
272 showcase the practical utility of our *enotetS* series promoters, we devised a single-plasmid-
273 based method for inducing synchronous meiosis.

274 Diploid *S. pombe* cells that are heterozygous for the mating type (*h+/h−*) can undergo
275 meiosis, whereas those that are homozygous for the mating type (*h+/h+* or *h−/h−*) cannot.
276 This is because the latter lack proteins encoded by one of the two types of mating-type
277 cassettes. In the case of *h+/h+* diploid cells, the missing proteins are the *matM*-cassette-
278 encoded proteins Mc and Mi (Kelly et al., 1988). In our new method for inducing meiosis, we
279 used *PenotetSW1* to induce the expression of Mc and Mi linked by a self-cleaving 2A peptide
280 (Mc-2A-Mi) in *h+/h+* diploid cells (Fig. 6A). *h+/h+* cells harboring an integration plasmid

281 expressing Mc-2A-Mi under the control of *PenotetSW1* were initially cultured in YES medium
282 and subsequently transferred to EMM−N medium to arrest the cells in G0. Following a 24-
283 hour incubation in EMM−N medium, ahTet was added to induce meiosis. Time course
284 analysis demonstrated the successful induction of synchronous meiosis (Fig. 6B). Tetrad
285 analysis revealed a spore viability of 97% for meiosis induced using this method (Fig. 6C).
286 Thus, we have established a new method for inducing meiosis that is characterized by good
287 synchrony and normal spore viability.
288

289 **Using *enotetS* series promoters to create conditional loss-of-function mutants**

290 Studying the functions of essential genes relies on the creation of conditional loss-of-function
291 mutants. Previously, we developed an auxin-inducible degron (AID) system for generating
292 such mutants in *S. pombe* (Zhang et al., 2022). However, not all genes are compatible with
293 the AID approach. In an unrelated project, we applied the AID method to construct conditional
294 loss-of-function mutants of three essential genes: *ypp1*, *sui1*, and *nrs1*. We first performed
295 endogenous AID tagging in a diploid background and obtained heterozygous tagged diploid
296 strains. Then, we attempted to derive haploid AID-tagged progeny through tetrad dissection
297 (Fig. S1). AID-tagged haploid progeny were readily obtained for *ypp1*. However, no viable
298 AID-tagged haploid progeny were obtained for *sui1* and *nrs1*, possibly due to AID tagging
299 interfering with the function of the protein products of these two genes. We decided to take
300 this opportunity to explore the feasibility of using the *enotetS* series promoters for generating
301 conditional loss-of-function mutants, especially for genes that are not amenable to the AID
302 approach.

303 We first separately deleted *sui1* and *nrs1* in a diploid background to obtain heterozygous
304 deletion diploid strains. Then, for each gene, a plasmid expressing the gene from
305 *PenotetSW2* and a plasmid expressing the gene from *PenotetSW3* were separately

306 integrated into the heterozygous deletion diploid strain. These two promoters were chosen
307 because their induced expression levels are close to the mRNA levels of *sui1* and *nrs1* in
308 vegetative cells (11 and 20 mRNA molecules per cell, respectively) (Marguerat et al., 2012;
309 Rutherford et al., 2024). The resulting strains were subjected to tetrad analysis on YES plates
310 with and without ahTet (Fig. 7). On YES plates without ahTet, for both genes, the basal level
311 expression from neither promoter was able to allow the deletion haploids to form colonies
312 (Fig. 7A). In contrast, on YES plates with ahTet, for both genes, the induced expression from
313 either promoter rescued the inviability of the deletion haploids (Fig. 7A). *PenotetSW2*-driven
314 induced expression in deletion haploids resulted in colony growth indistinguishable from wild
315 type, whereas *PenotetSW3*-driven induced expression resulted in colonies slightly smaller
316 than wild type at 3 days but not at 6 days (Fig. 7A). Thus, we successfully obtained
317 conditional lethal mutants for both genes.

318 To determine how quickly the loss-of-function phenotype arises upon the removal of
319 ahTet, we conducted a growth curve analysis (Fig. 7B). Haploid deletion strains harboring a
320 plasmid expressing the deleted gene from *PenotetSW2* or *PenotetSW3* were pre-cultured in
321 YES liquid medium with ahTet. After the cells were harvested and washed with water, they
322 were transferred to fresh YES medium with and without ahTet. At the six-hour time point, the
323 cultures in the ahTet-free YES medium started to exhibit a noticeably lower growth rate
324 compared to the cultures in the ahTet-containing YES medium. The differences in growth
325 rate became more pronounced as time elapsed. Given that the loss-of-function phenotype
326 does not manifest immediately after the promoter is turned off, but rather arises only after
327 the protein product has been significantly depleted through dilution and degradation, these
328 findings suggest that the *enotetS* series promoters can be rapidly switched off after shifting
329 cells to an ahTet-free medium. Therefore, these promoters provide useful tools for analyzing
330 loss-of-function phenotypes of essential genes in *S. pombe*.

Discussion

In this study, we have developed the *enotetS* series promoters, a new set of tetracycline-inducible promoters for *S. pombe*. These promoters offer a wide range of expression levels and allow for rapid induction of gene expression in both dividing and non-dividing cells. By combining each of these promoters with a TetR-expressing cassette, this system can be easily implemented in *S. pombe* through a single plasmid transformation. To demonstrate the usefulness of this new inducible expression system, we have successfully developed a new method for inducing synchronous meiosis and generated conditional loss-of-function mutants for two essential genes.

Tetracycline and its analogs have traditionally been considered biologically inert to eukaryotic physiology (Gossen et al., 1993). However, recent research has demonstrated that doxycycline, a commonly used inducer in mammalian tetracycline-inducible systems, disturbs mitochondrial protein translation, presumably due to the bacterial origin of mitochondria (Moullan et al., 2015). This raises concerns regarding the use of tetracycline-inducible systems (Chatzispyrou et al., 2015; De Boeck and Verfaillie, 2021; Ohira et al., 2017). Unlike tetracycline and doxycycline, which strongly inhibit bacterial protein translation and belong to the category of “classical tetracyclines”, the inducer used in our system, ahTet, does not effectively inhibit bacterial protein translation and is considered an “atypical tetracycline” (Rasmussen et al., 1991). Therefore, it is unlikely that ahTet negatively affects mitochondrial protein translation. Consistent with this, even though mitochondrial protein translation is essential for *S. pombe* proliferation, studies that have used ahTet on *S. pombe*, including our own, have not observed any detrimental effects on proliferation (Berg and Moseley, 2023; Erler et al., 2006; Lemay et al., 2014; Patterson et al., 2019; Shiroiwa et al., 2011; Sunder et al., 2012; Torres-Garcia et al., 2020; Wang et al., 2018; Zilio et al., 2012). As a precautionary measure against potential unknown side effects of ahTet on *S. pombe*,

356 especially when investigating non-growth phenotypes, we recommend including a strain
357 without an *enotetS* series promoter as a control to rule out the possibility that a phenotype is
358 caused by side effects of ahTet.

359 ahTet is a cost-effective inducer. When used at a concentration of 2.5 μg/ml, the cost of
360 ahTet for making one liter of ahTet-containing medium is about 6 US dollars (based on the
361 list price of Sigma-Aldrich catalog #37919). The ahTet-containing medium should be
362 prepared fresh from the DMSO-dissolved ahTet stock solution before use, as ahTet is not
363 very stable in aqueous solution. It has been reported that ahTet has a half-life of around 30
364 hours in culture media at 30°C (Politi et al., 2014).

365 The five induced expression levels of the *enotetS* series promoters offer a wide range
366 of possibilities for manipulating gene expression levels. In theory, even more intermediate
367 expression levels can be obtained by titrating the inducer dose. However, the *PenotetS*
368 promoter (and likely its weakened variants) exhibits a steep dose-response curve. This
369 means that the range of inducer doses over which the promoter is responsive, known as the
370 input dynamic range, is narrow. Consequently, precise adjustments to expression levels by
371 altering the inducer dose can be challenging (Azizoglu et al., 2021). If desired, the input
372 dynamic range can be expanded by implementing negative auto-regulation of tetR (Azizoglu
373 et al., 2021; Madar et al., 2011; Nevozhay et al., 2009; Patterson et al., 2019).

374 The use of the *enotetS* series promoters to generate conditional lethal mutants of
375 essential genes is a valuable alternative to the AID method, especially for genes that cannot
376 tolerate AID tagging. This strategy, known as promoter shut-off, has previously been
377 implemented in *S. pombe* using the *nmt1* series promoters and has successfully revealed
378 the loss-of-function phenotypes of many essential genes (Bestul et al., 2021; Kelly et al.,
379 1993; Matynia et al., 2002; Ottilie et al., 1995; Petersen and Hagan, 2003; Tajadura et al.,
380 2004; Wang et al., 2002; Westwood et al., 2004; Win et al., 2004; Yue et al., 2014). Compared

381 to the *nmt1* series promoters, the *enotetS* series promoters offer more levels of expression
382 and larger ratios between induced and repressed conditions. Therefore, they are expected
383 to be better tools for promoter shut-off.

384 While we generated the promoter shut-off strains for *sui1* and *nrs1* by first establishing
385 heterozygous deletion diploid strains and then deriving haploid strains, it should be feasible
386 to directly obtain promoter shut-off haploid strains by inserting an *enotetS* series promoter,
387 along with the TetR-expressing cassette, upstream of the target essential gene using a
388 single-step CRISPR-based marker-free knock-in (Jacobs et al., 2014; Zhang et al., 2018).
389 The intended knock-in clones can be readily selected based on their ability to grow on ahTet-
390 containing plates but not on ahTet-free plates. Promoter shut-off using the *nmt1* series
391 promoters can be initiated by simply adding thiamine to the culture, whereas promoter shut-
392 off using the *enotetS* series promoters requires the more laborious process of washing cells
393 to remove ahTet. It would be worth exploring in the future the feasibility of implementing the
394 method of light-induced inactivation of ahTet for shutting off the *enotetS* series promoters
395 (Baumschlager et al., 2020).
396

397 ## Materials and methods

398 ### Plasmid construction

399 The plasmids used in this study are listed in Table S1, and the primers used in this study are
400 listed in Table S2. We amplified the 276-bp *eno101* promoter (Wang et al., 2014) from
401 genomic DNA using primers oYY1 and oYY2. This amplified promoter was then cloned
402 between the SwaI and XhoI sites in the stable integration vector (SIV) pAV0714 (Addgene
403 plasmid 133479), replacing the *act1* promoter (Vještica et al., 2020). The resulting plasmid
404 was named pDB5530. For the construction of the *enotetS* promoter (*PenotetS*), a 19-bp
405 sequence between the TATA box and the transcription start site (TSS) of the *eno101*
406 promoter in pDB5530 was replaced with a 19-bp *tetO* sequence, specifically that of the O_2
407 operator from the bacterial transposon Tn*10* (TCCCTATCAGTGATAGAGA) (Hillen et al.,
408 1984, 1983; Wray and Reznikoff, 1983). This alteration was accomplished by performing
409 overlapping PCR using pDB5530 as the template and oXH5, oXH6, oXH7, and oXH8 as
410 primers, and then cloning the PCR product between the PacI and HpaI sites in pDB5530.
411 The resulting plasmid was named pDB5531. To use *PenotetS* to drive the expression of the
412 yellow fluorescent protein mECitrine, which serves as a reporter protein, we replaced the
413 *adh1* promoter in pDB4915, a modified SIV plasmid containing mECitrine, with *PenotetS*.
414 pDB4915 was derived from the SIV plasmid pAV0585 (pAde6^{PmeI}-hphMX, Addgene plasmid
415 133472) (Vještica et al., 2020), by altering the linearization site from PmeI to NotI and
416 introducing the *adh1* promoter, the coding sequence of mECitrine, and the terminator of the
417 *Saccharomyces cerevisiae ADH1* gene. *PenotetS* was amplified from pDB5531 using
418 primers oXH17 and oXH18, and then cloned between the ApaI and NheI sites in pDB4915.
419 The resulting plasmid was named pDB5532.

420 To construct an integration plasmid that contains both *PenotetS* and a TetR-expressing
421 cassette, we amplified a TetR expression cassette containing the cytomegalovirus promoter

422 (*P.CMV*) and the coding sequence of TetR from pDM291-tetR-tup11Δ70 (Addgene plasmid
423 41027) (Zilio et al., 2012), using primers oXH19 and oXH47. The amplified cassette was then
424 cloned into the KpnI site in pDB5532. The resulting plasmid was named pDB5318. To
425 construct weakened variants of *PenotetS*, we used primers oXH34-oXH38 to amplify four
426 PCR products, each containing *PenotetS* and a stem-loop-forming sequence immediately
427 downstream of *PenotetS*. These PCR products were then cloned separately between the
428 ApaI and NheI sites in pDB5318, generating four different plasmids, which were named
429 pDB5319-pDB5322. The four weakened variants of *PenotetS* in these four plasmids were
430 named *PenotetSW1*, *PenotetSW2*, *PenotetSW3*, and *PenotetSW4*. The plasmids pDB5318-
431 pDB5322 have been deposited at Addgene (Addgene plasmids 204828-204832) and the
432 Yeast Genetic Resource Center of Japan (YGRC/NBRP) (NBRP IDs FYP6242-6246). The
433 SnapGene files for these plasmids are provided in a compressed folder as a supplementary
434 file.

435 The DNA sequence encoding Mc-2A-Mi was synthesized by BGI Tech Solutions (Beijing
436 Liuhe) and consists of three parts: the coding sequence of Mi, a 60-bp segment encoding
437 the 20-amino acid T2A peptide (RAEGRGSLLTCGDVEENPGP) (Beekwilder et al., 2014),
438 and the coding sequence of Mc. To construct a plasmid expressing Mc-2A-Mi, the Mc-2A-Mi
439 sequence was amplified using primers oXH161 and oXH162, and then cloned between the
440 NheI and BglII sites of pDB5319, replacing the coding sequence of mECitrine. In the resulting
441 plasmid (pDB5533), Mc-2A-Mi is under the control of *PenotetSW1*.

442 The plasmids pDB4877, pDB4878, and pDB4879 were derived from the SIV vector
443 pAV0585 (pAde6^{PmeI}-hphMX, Addgene plasmid 133472) (Vještica et al., 2020), by altering
444 the linearization site from PmeI to NotI and introducing the *nmt1* promoter, the *41nmt1*
445 promoter, or the *81nmt1* promoter, respectively, along with the coding sequence of mECitrine,
446 and the terminator of the *Saccharomyces cerevisiae ADH1* gene. The plasmids pDB5534,

447 pDB5535, pDB5536, pDB5537, and pDB5538 were derived from the SIV plasmid pAV0586
448 (pLys3^{BstZ17I}-bsdMX, Addgene plasmid 133473), by altering the linearization site from
449 BstZ17I to NotI and introducing the TetR expression cassette, an *enotetS* series promoter,
450 the coding sequence of mECitrine, and the terminator of the *Saccharomyces cerevisiae*
451 *ADH1* gene. To construct plasmids expressing *nrs1*, the coding sequence of *nrs1* was
452 amplified from genomic DNA and cloned into pDB5537 and pDB5536, replacing the coding
453 sequence of mECitrine in each plasmid. The resulting plasmids were named pDB5539 and
454 pDB5541, respectively. Two plasmids expressing *sui1* were similarly constructed, except
455 cDNA was used as the amplification template, and they were named pDB5540 and pDB5542.
456

457 **Strain construction**

458 The *S. pombe* strains used in this study are listed in Table S3. Strains containing an
459 integrated plasmid were constructed by linearizing an SIV plasmid with NotI and then
460 transforming the plasmid into a host strain. Correct integration of the plasmid into the *ade6*
461 or *lys3* locus was verified using colony PCR (Vještica et al., 2020). Deletion strains were
462 created using PCR-based gene deletion. Strains with a gene endogenously tagged at the C-
463 terminus with the 3×sAID tag were generated through PCR-based gene tagging (Zhang et
464 al., 2022). The *h+/h−* diploid strain DY51002 was constructed by crossing two haploid strains
465 with *ade6-M210* and *ade6-M216* mutations, respectively. The two haploid strains were pre-
466 grown on YES plates and then mixed in an equal ratio in 20 μL of water. The mixture was
467 spotted on SPA plates with necessary supplements. After approximately 12 hours of
468 incubation at 30°C, cells were collected and plated on YE plates containing 200 mg/L guanine
469 at a density of approximately 10^4 cells per plate. Guanine was used to inhibit the uptake of
470 adenine, thereby preventing the growth of adenine auxotrophs and allowing only the growth
471 of *ade6-M210*/*ade6-M216* diploid cells, which are adenine prototrophs due to interallelic

472 complementation (Cummins and Mitchison, 1967; Smith, 2009). After incubating for 3 days
473 at 30°C, colonies formed on the guanine-containing plates were streaked on YE2A plates. A
474 diploid clone that showed high spore viability in tetrad analysis was saved as DY51002. A
475 prototrophic *h+/h−* diploid strain, DY50999, constructed in the same way as DY51002, was
476 plated on YEPD plates, and colonies that were unable to form spores were selected based
477 on iodine staining. The mating type of the non-sporulating diploid clones was determined by
478 colony PCR, and an *h+/h+* diploid strain was saved as DY51000.
479
480 **Media and growth conditions**
481 The compositions of the media were as described (Petersen and Russell, 2016).
482 Anhydrotetracycline hydrochloride (ahTet; J&K Scientific, catalog number 541642) was
483 dissolved in DMSO at a concentration of 5 mg/ml and stored at −80°C.
484 To analyze the dose response of the inducer, the cells were first cultured in liquid YES
485 medium or EMM medium with the necessary supplements until they reached the logarithmic
486 phase. The DMSO-diluted ahTet stock was then added to achieve the desired concentrations,
487 with an equal volume of DMSO serving as the control. After 24 hours of culturing (with
488 cultures diluted when the OD600 approaching 1.0) at 30°C, logarithmic phase cells were
489 collected for live-cell imaging.
490 For the time course assay of proliferating cells, the cells were first cultured in liquid YES
491 medium or EMM medium with the necessary supplements until they reached the logarithmic
492 phase at 30°C. After adding ahTet to the medium, the cells were collected at specific time
493 points. During the time course, the cultures were diluted when the OD600 approached 1.0.
494 To quantify the expression levels of the *enotetS* series promoters, induced expression
495 levels were measured after transferring logarithmic phase cells to media with 2.5 μg/ml ahTet
496 for 24 hours at 30°C. Repressed expression levels were measured after transfer to media

497 with DMSO under the same conditions.

498 To quantify the expression levels of the *nmt1* series promoters, the cells were first
499 cultured in EMM medium containing thiamine until they reached the logarithmic phase. Then,
500 to measure the induced expression levels, the cells were washed three times with water,
501 transferred to EMM medium without thiamine, and grown at 30°C for 24 hours. To measure
502 the repressed expression levels, the cells were cultured in EMM medium containing thiamine
503 at 30°C for 24 hours.

504 For the time course assay of G0 phase cells, logarithmically growing cells grown in EMM
505 medium were washed three times with water and shifted to EMM medium without nitrogen
506 (EMM−N) for 24 hours at 30°C to arrest the cells in the G0 phase. After adding ahTet to the
507 medium at a concentration of 2.5 μg/ml, the cells were collected at specific time points.

508 For the time course assay of spores, h^{90} cells grown in YES medium were washed three
509 times with water and shifted to MSL−N medium at 30°C for 48 hours to induce sporulation.
510 Then, the cells were collected and treated with Snailase (Beijing Solarbio Science &
511 Technology Co.,Ltd., catalog number S8280) in water at 30°C for 24 hours to digest non-
512 spore cells. After digestion, spores were purified by centrifugation in Percoll solutions. Spores
513 were incubated in EMM−N medium overnight. Then ahTet was added to the EMM−N medium.
514 After adding ahTet to the medium at a concentration of 2.5 μg/ml, spores were collected at
515 specific time points.

516 For the growth curve analysis, haploid deletion strains harboring a plasmid expressing
517 the deleted gene from *PenotetSW2* or *PenotetSW3*, along with a wild-type strain were pre-
518 cultured in YES liquid medium supplemented with ahTet until they reached the logarithmic
519 phase at 30°C. Then, the cells were washed three times with water and transferred to either
520 YES medium or YES medium supplemented with ahTet. The optical density at 600 nm
521 (OD600) of each culture was measured at specific time points, with cultures being diluted if

522 the OD600 approached 1.0. The number of generations was determined based on the
523 OD600 and the dilution ratio.
524
525 **Fluorescence microscopy and image quantification**
526 Live-cell imaging was performed using a Dragonfly 200 spinning disk confocal microscope
527 system (Andor Technology) equipped with an mCherry/YFP/CFP filter set and an
528 mCherry/GFP filter set. Images were acquired with a 100×, 1.4-NA objective using a Sona
529 sCMOS camera and analyzed with Fiji (ImageJ).
530 To quantify the expression level of mECitrine, first, channels of images were split and
531 the DIC channel was used to segment cell boundaries using Cellpose (version 2.1.1)
532 (Stringer et al., 2021). The resulting masked images were processed with the LabelsToRois
533 plugin (Waisman et al., 2021) in Fiji (Schindelin et al., 2012). This plugin generated outlines
534 outlining the boundaries of each cell. Subsequently, the generated outlines were
535 superimposed onto the mECitrine channel. Fiji was employed to calculate the mean
536 fluorescence intensity for each individual cell.
537 In total, three images were acquired for each sample, with each image containing
538 between 50 and 200 cells. The median fluorescence intensity of cells within each image was
539 calculated and averaged across the triplicate images. Background fluorescence was
540 measured using a parental strain that lacked mECitrine and was subsequently subtracted.
541 The resulting fluorescence intensity provided a measurement of the expression level.
542
543 **Induction and monitoring of meiosis**
544 Log-phase cells grown in YES medium were collected, washed three times with water,
545 resuspended in EMM medium without nitrogen (EMM−N), and incubated at 30°C for 24 hours
546 to arrest cells in the G0 phase. Then, ahTet was added to the culture at a final concentration

547 of 2.5 μg/ml to induce meiosis. At specific time points, cells were collected and fixed using
548 70% ethanol. The advancement of meiosis was evaluated by quantifying the number of nuclei
549 per cell after staining the DNA with SYTOX Green (Thermo Fisher, catalog number S7020).
550 For SYTOX Green staining, the fixed cells were washed once with water, resuspended in
551 water containing 1 μM SYTOX Green, and incubated in the dark at room temperature for 5
552 minutes. The number of nuclei per cell was determined through imaging.
553
554 **Tetrad analysis**
555 To examine spore viability of induced meiosis, cells collected 24 hours after meiosis induction
556 were streaked onto YES plates. Tetrad analysis was carried out using a TDM50 tetrad
557 dissection microscope (Micro Video Instruments, Avon, USA) on YES plates. To assess
558 whether the exogenous expression of *nrs1* or *sui1* can complement the deletion of the
559 corresponding endogenous gene, diploid strains freshly grown on YE2A plates were spotted
560 onto SPASK plates. The SPASK plates were incubated at 30°C for about 24 h. Subsequently,
561 tetrad analysis was carried out on YES plates with and without ahTet.
562

Acknowledgements

We thank the Sophie Martin laboratory for making the SIV plasmids they have developed available through Addgene and the Yeast Genetic Resource Center of Japan (YGRC/NBRP). We thank YGRC/NBRP for providing the plasmids.

Competing interests

No competing interests declared.

Funding

This work was supported by funding from the Ministry of Science and Technology of the People's Republic of China, the Beijing municipal government, and Tsinghua University.

References

Amelina, H., Moiseeva, V., Collopy, L.C., Pearson, S.R., Armstrong, C.A., Tomita, K. (2016). Sequential and counter-selectable cassettes for fission yeast. BMC Biotechnol 16, 76. https://doi.org/10.1186/s12896-016-0307-4

Azizoglu, A., Brent, R., Rudolf, F. (2021). A precisely adjustable, variation-suppressed eukaryotic transcriptional controller to enable genetic discovery. Elife 10, e69549. https://doi.org/10.7554/eLife.69549

Bähler, J., Schuchert, P., Grimm, C., Kohli, J. (1991). Synchronized meiosis and recombination in fission yeast: observations with pat1-114 diploid cells. Curr Genet 19, 445–451. https://doi.org/10.1007/BF00312735

Basi, G., Schmid, E., Maundrell, K. (1993). TATA box mutations in the Schizosaccharomyces pombe nmt1 promoter affect transcription efficiency but not the transcription start point or thiamine repressibility. Gene 123, 131–136. https://doi.org/10.1016/0378-1119(93)90552-E

Baumschlager, A., Rullan, M., Khammash, M. (2020). Exploiting natural chemical photosensitivity of anhydrotetracycline and tetracycline for dynamic and setpoint chemo-optogenetic control. Nat Commun 11, 3834. https://doi.org/10.1038/s41467-020-17677-5

Beekwilder, J., van Rossum, H.M., Koopman, F., Sonntag, F., Buchhaupt, M., Schrader, J., Hall, R.D., Bosch, D., Pronk, J.T., van Maris, A.J.A., Daran, J.-M. (2014). Polycistronic expression of a β-carotene biosynthetic pathway in Saccharomyces cerevisiae coupled to β-ionone production. J Biotechnol 192 Pt B, 383–392. https://doi.org/10.1016/j.jbiotec.2013.12.016

Bellemare, D.R., Sanschagrin, M., Beaudoin, J., Labbé, S. (2001). A novel copper-regulated promoter system for expression of heterologous proteins in Schizosaccharomyces pombe. Gene 273, 191–198. https://doi.org/10.1016/s0378-1119(01)00591-1

Bellí, G., Garí, E., Piedrafita, L., Aldea, M., Herrero, E. (1998). An activator/repressor dual system allows tight tetracycline-regulated gene expression in budding yeast. Nucleic Acids Res 26, 942–947. https://doi.org/10.1093/nar/26.4.942

Berens, C., Hillen, W. (2003). Gene regulation by tetracyclines. Constraints of resistance regulation in bacteria shape TetR for application in eukaryotes. Eur J Biochem 270, 3109–3121. https://doi.org/10.1046/j.1432-1033.2003.03694.x

Berg, R.A., Moseley, J.B. (2023). Regulation of cell size and Wee1 kinase by elevated levels of the cell cycle regulatory protein kinase Cdr2. J Biol Chem 299, 102831. https://doi.org/10.1016/j.jbc.2022.102831

Bestul, A.J., Yu, Z., Unruh, J.R., Jaspersen, S.L. (2021). Redistribution of

611 centrosomal proteins by centromeres and Polo kinase controls partial nuclear envelope
612 breakdown in fission yeast. Mol Biol Cell 32, 1487–1500.
613 https://doi.org/10.1091/mbc.E21-05-0239
614 **Chatzispyrou, I.A., Held, N.M., Mouchiroud, L., Auwerx, J., Houtkooper, R.H.**
615 (2015). Tetracycline antibiotics impair mitochondrial function and its experimental use
616 confounds research. Cancer Res 75, 4446–4449. https://doi.org/10.1158/0008-
617 5472.CAN-15-1626
618 **Chikashige, Y., Kurokawa, R., Haraguchi, T., Hiraoka, Y.** (2004). Meiosis induced
619 by inactivation of Pat1 kinase proceeds with aberrant nuclear positioning of
620 centromeres in the fission yeast Schizosaccharomyces pombe. Genes Cells 9, 671–684.
621 https://doi.org/10.1111/j.1356-9597.2004.00760.x
622 **Cipak, L., Hyppa, R.W., Smith, G.R., Gregan, J.** (2012). ATP analog-sensitive Pat1
623 protein kinase for synchronous fission yeast meiosis at physiological temperature. Cell
624 Cycle 11, 1626–1633. https://doi.org/10.4161/cc.20052
625 **Corish, P., Tyler-Smith, C.** (1999). Attenuation of green fluorescent protein half-life
626 in mammalian cells. Protein Eng 12, 1035–1040.
627 https://doi.org/10.1093/protein/12.12.1035
628 **Cummins, J.E., Mitchison, J.M.** (1967). Adenine uptake and pool formation in the
629 fission yeast Schizosaccharomyces pombe. Biochim Biophys Acta 136, 108–120.
630 https://doi.org/10.1016/0304-4165(67)90326-1
631 **De Boeck, J., Verfaillie, C.** (2021). Doxycycline inducible overexpression systems:
632 how to induce your gene of interest without inducing misinterpretations. Mol Biol Cell
633 32, 1517–1522. https://doi.org/10.1091/mbc.E21-04-0177
634 **Erler, A., Maresca, M., Fu, J., Stewart, A.F.** (2006). Recombineering reagents for
635 improved inducible expression and selection marker re-use in Schizosaccharomyces
636 pombe. Yeast 23, 813–823. https://doi.org/10.1002/yea.1396
637 **Faryar, K., Gatz, C.** (1992). Construction of a Tetracycline-inducible promoter in
638 Schizosaccharomyces pombe. Curr Genet 21, 345–349.
639 https://doi.org/10.1007/BF00351693
640 **Forsburg, S.L.** (1993). Comparison of Schizosaccharomyces pombe expression
641 systems. Nucleic Acids Res 21, 2955–2956. https://doi.org/10.1093/nar/21.12.2955
642 **Fujita, Y., Tohda, H., Giga-Hama, Y., Takegawa, K.** (2006). Heat shock-inducible
643 expression vectors for use in Schizosaccharomyces pombe. FEMS Yeast Res 6, 883–
644 887. https://doi.org/10.1111/j.1567-1364.2006.00093.x
645 **Garg, A.** (2020). A lncRNA-regulated gene expression system with rapid induction
646 kinetics in the fission yeast Schizosaccharomyces pombe. RNA 26, 1743–1752.
647 https://doi.org/10.1261/rna.076000.120

Garí, E., Piedrafita, L., Aldea, M., Herrero, E. (1997). A set of vectors with a tetracycline-regulatable promoter system for modulated gene expression in Saccharomyces cerevisiae. Yeast 13, 837–848. https://doi.org/10.1002/(SICI)1097-0061(199707)13:9<837::AID-YEA145>3.0.CO;2-T

Gossen, M., Bonin, A.L., Bujard, H. (1993). Control of gene activity in higher eukaryotic cells by prokaryotic regulatory elements. Trends Biochem Sci 18, 471–475. https://doi.org/10.1016/0968-0004(93)90009-c

Guerra-Moreno, A., Alves-Rodrigues, I., Hidalgo, E., Ayté, J. (2012). Chemical genetic induction of meiosis in Schizosaccharomyces pombe. Cell Cycle 11, 1621–1625. https://doi.org/10.4161/cc.20051

He, L., Binari, R., Huang, J., Falo-Sanjuan, J., Perrimon, N. (2019). In vivo study of gene expression with an enhanced dual-color fluorescent transcriptional timer. Elife 8, e46181. https://doi.org/10.7554/eLife.46181

Hennig, S., Hornauer, N., Rödel, G., Ostermann, K. (2018). Pheromone-inducible expression vectors for fission yeast Schizosaccharomyces pombe. Plasmid 95, 1–6. https://doi.org/10.1016/j.plasmid.2017.11.002

Hillen, W., Gatz, C., Altschmied, L., Schollmeier, K., Meier, I. (1983). Control of expression of the Tn10-encoded tetracycline resistance genes. Equilibrium and kinetic investigation of the regulatory reactions. J Mol Biol 169, 707–721. https://doi.org/10.1016/s0022-2836(83)80166-1

Hillen, W., Schollmeier, K., Gatz, C. (1984). Control of expression of the Tn10-encoded tetracycline resistance operon. II. Interaction of RNA polymerase and TET repressor with the tet operon regulatory region. J Mol Biol 172, 185–201. https://doi.org/10.1016/s0022-2836(84)80037-6

Hoffman, C.S., Winston, F. (1989). A transcriptionally regulated expression vector for the fission yeast Schizosaccharomyces pombe. Gene 84, 473–479. https://doi.org/10.1016/0378-1119(89)90523-4

Iacovoni, J.S., Russell, P., Gaits, F. (1999). A new inducible protein expression system in fission yeast based on the glucose-repressed inv1 promoter. Gene 232, 53–58. https://doi.org/10.1016/S0378-1119(99)00116-X

Iino, Y., Yamamoto, M. (1985). Negative control for the initiation of meiosis in Schizosaccharomyces pombe. Proc Natl Acad Sci U S A 82, 2447–2451. https://doi.org/10.1073/pnas.82.8.2447

Jacobs, J.Z., Ciccaglione, K.M., Tournier, V., Zaratiegui, M. (2014). Implementation of the CRISPR-Cas9 system in fission yeast. Nat Commun 5, 5344. https://doi.org/10.1038/ncomms6344

Kelly, M., Burke, J., Smith, M., Klar, A., Beach, D. (1988). Four mating-type genes

control sexual differentiation in the fission yeast. EMBO J 7, 1537–1547.
Kelly, T.J., Martin, G.S., Forsburg, S.L., Stephen, R.J., Russo, A., Nurse, P. (1993). The fission yeast cdc18+ gene product couples S phase to START and mitosis. Cell 74, 371–382. https://doi.org/10.1016/0092-8674(93)90427-r
Kjaerulff, S., Nielsen, O. (2015). An IPTG-inducible derivative of the fission yeast nmt promoter. Yeast 32, 469–478. https://doi.org/10.1002/yea.3073
Kumar, R., Singh, J. (2006). A truncated derivative of nmt 1 promoter exhibits temperature-dependent induction of gene expression in Schizosaccharomyces pombe. Yeast 23, 55–65. https://doi.org/10.1002/yea.1343
Lamping, E., Niimi, M., Cannon, R.D. (2013). Small, synthetic, GC-rich mRNA stem-loop modules 5' proximal to the AUG start-codon predictably tune gene expression in yeast. Microb Cell Fact 12, 74. https://doi.org/10.1186/1475-2859-12-74
Lemay, J.-F., Larochelle, M., Marguerat, S., Atkinson, S., Bähler, J., Bachand, F. (2014). The RNA exosome promotes transcription termination of backtracked RNA polymerase II. Nat Struct Mol Biol 21, 919–926. https://doi.org/10.1038/nsmb.2893
Li, H., Hou, J., Bai, L., Hu, C., Tong, P., Kang, Y., Zhao, X., Shao, Z. (2015). Genome-wide analysis of core promoter structures in Schizosaccharomyces pombe with DeepCAGE. RNA Biol 12, 525–537. https://doi.org/10.1080/15476286.2015.1022704
Lu, Z., Lin, Z. (2021). The origin and evolution of a distinct mechanism of transcription initiation in yeasts. Genome Res 31, 51–63. https://doi.org/10.1101/gr.264325.120
Madar, D., Dekel, E., Bren, A., Alon, U. (2011). Negative auto-regulation increases the input dynamic-range of the arabinose system of Escherichia coli. BMC Syst Biol 5, 111. https://doi.org/10.1186/1752-0509-5-111
Marguerat, S., Schmidt, A., Codlin, S., Chen, W., Aebersold, R., Bähler, J. (2012). Quantitative analysis of fission yeast transcriptomes and proteomes in proliferating and quiescent cells. Cell 151, 671–683. https://doi.org/10.1016/j.cell.2012.09.019
Matsuzawa, T., Tohda, H., Takegawa, K. (2013). Ethanol-inducible gene expression using gld1 (+) promoter in the fission yeast Schizosaccharomyces pombe. Appl Microbiol Biotechnol 97, 6835–6843. https://doi.org/10.1007/s00253-013-4812-2
Matynia, A., Salus, S.S., Sazer, S. (2002). Three proteins required for early steps in the protein secretory pathway also affect nuclear envelope structure and cell cycle progression in fission yeast. J Cell Sci 115, 421–431. https://doi.org/10.1242/jcs.115.2.421
Maundrell, K. (1993). Thiamine-repressible expression vectors pREP and pRIP for fission yeast. Gene 123, 127–130. https://doi.org/10.1016/0378-1119(93)90551-d
Maundrell, K. (1990). nmt1 of fission yeast. A highly transcribed gene completely

722 repressed by thiamine. Journal of Biological Chemistry 265, 10857–10864.
723 https://doi.org/10.1016/S0021-9258(19)38525-4
724 **Moreno, M.B., Durán, A., Ribas, J.C.** (2000). A family of multifunctional thiamine-
725 repressible expression vectors for fission yeast. Yeast 16, 861–872.
726 https://doi.org/10.1002/1097-0061(20000630)16:9<861::AID-YEA577>3.0.CO;2-9
727 **Moullan, N., Mouchiroud, L., Wang, X., Ryu, D., Williams, E.G., Mottis, A.,**
728 **Jovaisaite, V., Frochaux, M.V., Quiros, P.M., Deplancke, B., Houtkooper, R.H.,**
729 **Auwerx, J.** (2015). Tetracyclines Disturb Mitochondrial Function across Eukaryotic
730 Models: A Call for Caution in Biomedical Research. Cell Rep 10, 1681–1691.
731 https://doi.org/10.1016/j.celrep.2015.02.034
732 **Murphy, K.F., Balázsi, G., Collins, J.J.** (2007). Combinatorial promoter design for
733 engineering noisy gene expression. Proc Natl Acad Sci U S A 104, 12726–12731.
734 https://doi.org/10.1073/pnas.0608451104
735 **Nevozhay, D., Adams, R.M., Murphy, K.F., Josic, K., Balázsi, G.** (2009). Negative
736 autoregulation linearizes the dose-response and suppresses the heterogeneity of gene
737 expression. Proc Natl Acad Sci U S A 106, 5123–5128.
738 https://doi.org/10.1073/pnas.0809901106
739 **Ohira, M.J., Hendrickson, D.G., Scott McIsaac, R., Rhind, N.** (2017). An estradiol-
740 inducible promoter enables fast, graduated control of gene expression in fission yeast.
741 Yeast 34, 323–334. https://doi.org/10.1002/yea.3235
742 **Ottilie, S., Miller, P.J., Johnson, D.I., Creasy, C.L., Sells, M.A., Bagrodia, S.,**
743 **Forsburg, S.L., Chernoff, J.** (1995). Fission yeast pak1+ encodes a protein kinase that
744 interacts with Cdc42p and is involved in the control of cell polarity and mating. EMBO
745 J 14, 5908–5919. https://doi.org/10.1002/j.1460-2075.1995.tb00278.x
746 **Patterson, J.O., Rees, P., Nurse, P.** (2019). Noisy Cell-Size-Correlated Expression of
747 Cyclin B Drives Probabilistic Cell-Size Homeostasis in Fission Yeast. Current Biology
748 29, 1379-1386.e4. https://doi.org/10.1016/j.cub.2019.03.011
749 **Perruca-Foncillas, R., Davidsson, J., Carlquist, M., Gorwa-Grauslund, M.F.**
750 (2022). Assessment of fluorescent protein candidates for multi-color flow cytometry
751 analysis of Saccharomyces cerevisiae. Biotechnol Rep (Amst) 34, e00735.
752 https://doi.org/10.1016/j.btre.2022.e00735
753 **Petersen, J., Hagan, I.M.** (2003). S. pombe aurora kinase/survivin is required for
754 chromosome condensation and the spindle checkpoint attachment response. Curr Biol
755 13, 590–597. https://doi.org/10.1016/s0960-9822(03)00205-7
756 **Petersen, J., Russell, P.** (2016). Growth and the Environment of Schizosaccharomyces
757 pombe. Cold Spring Harb Protoc 2016, pdb.top079764.
758 https://doi.org/10.1101/pdb.top079764

Picard, D., Schena, M., Yamamoto, K.R. (1990). An inducible expression vector for both fission and budding yeast. Gene 86, 257–261. https://doi.org/10.1016/0378-1119(90)90287-2

Politi, N., Pasotti, L., Zucca, S., Casanova, M., Micoli, G., Cusella De Angelis, M.G., Magni, P. (2014). Half-life measurements of chemical inducers for recombinant gene expression. J Biol Eng 8, 5. https://doi.org/10.1186/1754-1611-8-5

Rasmussen, B., Noller, H.F., Daubresse, G., Oliva, B., Misulovin, Z., Rothstein, D.M., Ellestad, G.A., Gluzman, Y., Tally, F.P., Chopra, I. (1991). Molecular basis of tetracycline action: identification of analogs whose primary target is not the bacterial ribosome. Antimicrob Agents Chemother 35, 2306–2311. https://doi.org/10.1128/AAC.35.11.2306

Rosenfeld, N., Elowitz, M.B., Alon, U. (2002). Negative autoregulation speeds the response times of transcription networks. J Mol Biol 323, 785–793. https://doi.org/10.1016/s0022-2836(02)00994-4

Russell, P.R. (1983). Evolutionary divergence of the mRNA transcription initiation mechanism in yeast. Nature 301, 167–169. https://doi.org/10.1038/301167a0

Rutherford, K.M., Lera-Ramírez, M., Wood, V. (2024). PomBase: a Global Core Biodata Resource-growth, collaboration, and sustainability. Genetics 227, iyae007. https://doi.org/10.1093/genetics/iyae007

Schindelin, J., Arganda-Carreras, I., Frise, E., Kaynig, V., Longair, M., Pietzsch, T., Preibisch, S., Rueden, C., Saalfeld, S., Schmid, B., Tinevez, J.-Y., White, D.J., Hartenstein, V., Eliceiri, K., Tomancak, P., Cardona, A. (2012). Fiji: an open-source platform for biological-image analysis. Nat Methods 9, 676–682. https://doi.org/10.1038/nmeth.2019

Shiroiwa, Y., Hayashi, T., Fujita, Y., Villar-Briones, A., Ikai, N., Takeda, K., Ebe, M., Yanagida, M. (2011). Mis17 is a regulatory module of the Mis6-Mal2-Sim4 centromere complex that is required for the recruitment of CenH3/CENP-A in fission yeast. PLoS One 6, e17761. https://doi.org/10.1371/journal.pone.0017761

Smith, G.R. (2009). Genetic Analysis of Meiotic Recombination in Schizosaccharomyces pombe. Methods Mol Biol 557, 65–76.

Stringer, C., Wang, T., Michaelos, M., Pachitariu, M. (2021). Cellpose: a generalist algorithm for cellular segmentation. Nat Methods 18, 100–106. https://doi.org/10.1038/s41592-020-01018-x

Sunder, S., Greeson-Lott, N.T., Runge, K.W., Sanders, S.L. (2012). A new method to efficiently induce a site-specific double-strand break in the fission yeast Schizosaccharomyces pombe. Yeast 29, 275–291. https://doi.org/10.1002/yea.2908

Tajadura, V., García, B., García, I., García, P., Sánchez, Y. (2004).

796 Schizosaccharomyces pombe Rgf3p is a specific Rho1 GEF that regulates cell wall
797 beta-glucan biosynthesis through the GTPase Rho1p. J Cell Sci 117, 6163–6174.
798 https://doi.org/10.1242/jcs.01530
799 **Thodberg, M., Thieffry, A., Bornholdt, J., Boyd, M., Holmberg, C., Azad, A.,**
800 **Workman, C.T., Chen, Y., Ekwall, K., Nielsen, O., Sandelin, A.** (2019).
801 Comprehensive profiling of the fission yeast transcription start site activity during stress
802 and media response. Nucleic Acids Res 47, 1671–1691.
803 https://doi.org/10.1093/nar/gky1227
804 **Tommasino, M., Maundrell, K.** (1991). Uptake of thiamine by Schizosaccharomyces
805 pombe and its effect as a transcriptional regulator of thiamine-sensitive genes. Curr
806 Genet 20, 63–66. https://doi.org/10.1007/BF00312766
807 **Torres-Garcia, S., Yaseen, I., Shukla, M., Audergon, P.N.C.B., White, S.A.,**
808 **Pidoux, A.L., Allshire, R.C.** (2020). Epigenetic gene silencing by heterochromatin
809 primes fungal resistance. Nature 585, 453–458. https://doi.org/10.1038/s41586-020-
810 2706-x
811 **Toyama, R., Okayama, H.** (1990). Human chorionic gonadotropin alpha and human
812 cytomegalovirus promoters are extremely active in the fission yeast
813 Schizosaccharomyces pombe. FEBS Lett 268, 217–221. https://doi.org/10.1016/0014-
814 5793(90)81012-d
815 **Vještica, A., Marek, M., Nkosi, P.J., Merlini, L., Liu, G., Bérard, M., Billault-**
816 **Chaumartin, I., Martin, S.G.** (2020). A toolbox of stable integration vectors in the
817 fission yeast Schizosaccharomyces pombe. Journal of Cell Science 133, jcs240754.
818 https://doi.org/10.1242/jcs.240754
819 **Waisman, A., Norris, A.M., Elías Costa, M., Kopinke, D.** (2021). Automatic and
820 unbiased segmentation and quantification of myofibers in skeletal muscle. Sci Rep 11,
821 11793. https://doi.org/10.1038/s41598-021-91191-6
822 **Wang, H., Tang, X., Liu, J., Trautmann, S., Balasundaram, D., McCollum, D.,**
823 **Balasubramanian, M.K.** (2002). The multiprotein exocyst complex is essential for cell
824 separation in Schizosaccharomyces pombe. Mol Biol Cell 13, 515–529.
825 https://doi.org/10.1091/mbc.01-11-0542
826 **Wang, Hongcheng, Wang, Haiyang, Wang, M., Zhang, L., Wang, R., Mei, Y.,**
827 **Shao, W.** (2014). Identification and refinement of two strong constitutive promoters for
828 gene expression system of Schizosaccharomyces pombe. World J Microbiol Biotechnol
829 30, 1809–1817. https://doi.org/10.1007/s11274-014-1603-6
830 **Wang, J., Eisenstatt, J.R., Audry, J., Cornelius, K., Shaughnessy, M., Berkner,**
831 **K.L., Runge, K.W.** (2018). A Heterochromatin Domain Forms Gradually at a New
832 Telomere and Is Dynamic at Stable Telomeres. Mol Cell Biol 38, e00393-17.

833 https://doi.org/10.1128/MCB.00393-17
834 **Watson, A.T., Werler, P., Carr, A.M.** (2011). Regulation of gene expression at the
835 fission yeast Schizosaccharomyces pombe urg1 locus. Gene 484, 75–85.
836 https://doi.org/10.1016/j.gene.2011.05.028
837 **Watt, S., Mata, J., López-Maury, L., Marguerat, S., Burns, G., Bähler, J.** (2008).
838 urg1: A Uracil-Regulatable Promoter System for Fission Yeast with Short Induction
839 and Repression Times. PLOS ONE 3, e1428.
840 https://doi.org/10.1371/journal.pone.0001428
841 **Westwood, P.K., Martin, I.V., Fantes, P.A.** (2004). Fission yeast Cdc37 is required
842 for multiple cell cycle functions. Mol Genet Genomics 271, 82–90.
843 https://doi.org/10.1007/s00438-003-0958-4
844 **Win, T.Z., Goodwin, A., Hickson, I.D., Norbury, C.J., Wang, S.-W.** (2004).
845 Requirement for Schizosaccharomyces pombe Top3 in the maintenance of chromosome
846 integrity. J Cell Sci 117, 4769–4778. https://doi.org/10.1242/jcs.01351
847 **Wray, L.V., Reznikoff, W.S.** (1983). Identification of repressor binding sites
848 controlling expression of tetracycline resistance encoded by Tn10. J Bacteriol 156,
849 1188–1191. https://doi.org/10.1128/jb.156.3.1188-1191.1983
850 **Yamamoto, A., Hiraoka, Y.** (2003). Monopolar spindle attachment of sister
851 chromatids is ensured by two distinct mechanisms at the first meiotic division in fission
852 yeast. The EMBO Journal 22, 2284–2296. https://doi.org/10.1093/emboj/cdg222
853 **Yue, M., Zeng, L., Singh, A., Xu, Y.** (2014). Rad4 mainly functions in Chk1-mediated
854 DNA damage checkpoint pathway as a scaffold protein in the fission yeast
855 Schizosaccharomyces pombe. PLoS One 9, e92936.
856 https://doi.org/10.1371/journal.pone.0092936
857 **Zhang, X.-R., He, J.-B., Wang, Y.-Z., Du, L.-L.** (2018). A Cloning-Free Method for
858 CRISPR/Cas9-Mediated Genome Editing in Fission Yeast. G3 (Bethesda) 8, 2067–
859 2077. https://doi.org/10.1534/g3.118.200164
860 **Zhang, X.-R., Zhao, L., Suo, F., Gao, Y., Wu, Q., Qi, X., Du, L.-L.** (2022). An
861 improved auxin-inducible degron system for fission yeast. G3 Genes|Genomes|Genetics
862 12, jkab393. https://doi.org/10.1093/g3journal/jkab393
863 **Zilio, N., Wehrkamp-Richter, S., Boddy, M.N.** (2012). A new versatile system for
864 rapid control of gene expression in the fission yeast Schizosaccharomyces pombe. Yeast
865 29, 425–434. https://doi.org/10.1002/yea.2920
866

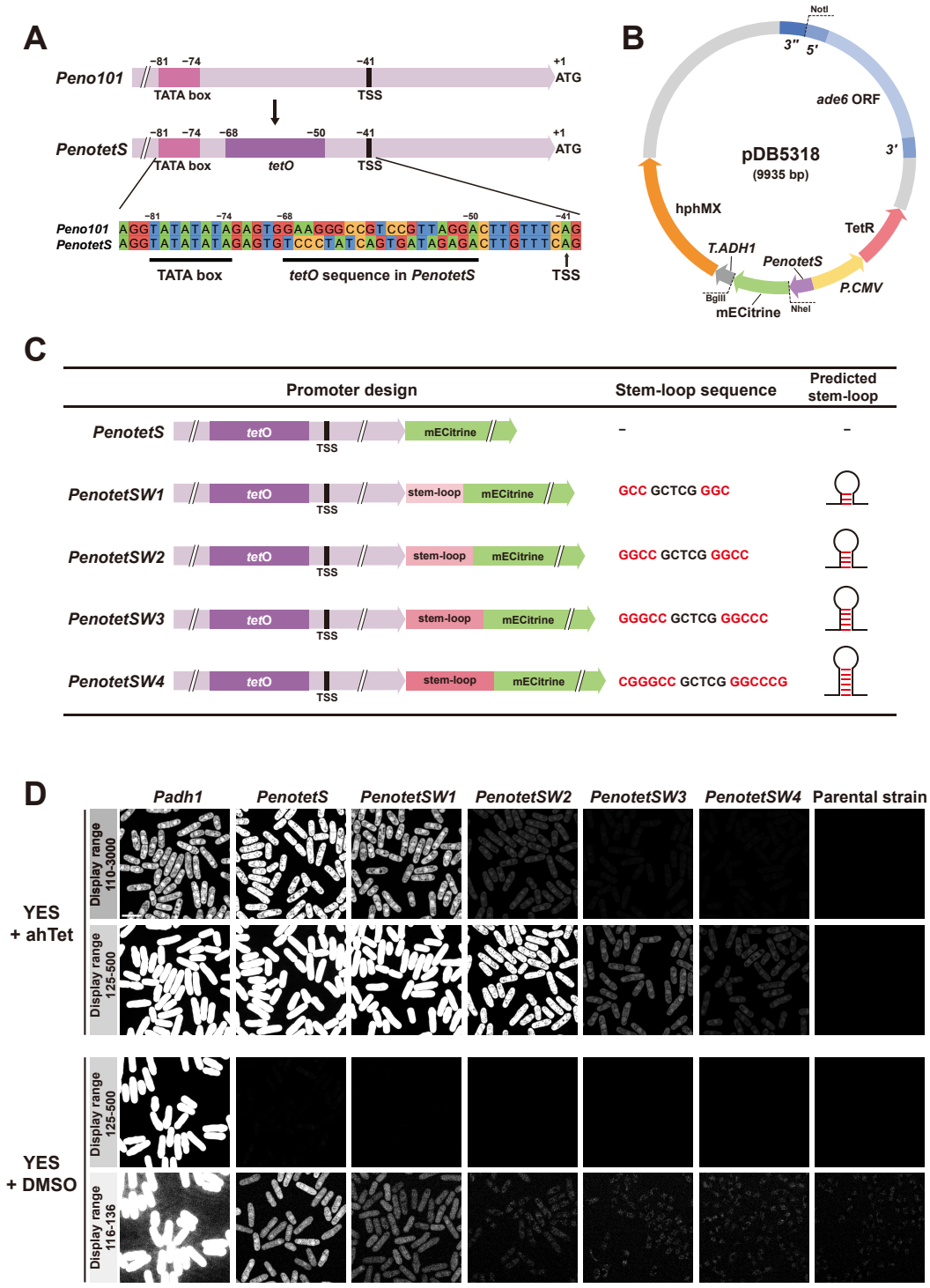

Fig. 1. Overview of the new tetracycline-inducible expression system.

(A) Schematic showing how the *enotetS* promoter (*PenotetS*) was generated. *PenotetS*

was engineered from the *eno101* promoter (*Peno101*) by introducing a single 19-bp *tetO* sequence between the TATA box and the transcription start site (TSS) of *Peno101*, while maintaining the original distance between the TATA box and the TSS.

(B) Diagram of the integration plasmid pDB5318. This plasmid contains *PenotetS* and a TetR-expressing cassette, which consists of the cytomegalovirus promoter (*P.CMV*) and the TetR coding sequence. The plasmid can be integrated at the *ade6* locus following linearization with NotI digestion. The mECitrine coding sequence can be replaced with the sequence of any desired gene to be expressed under the control of *PenotetS*, using the NheI and BglII restriction sites.

(C) Schematic of four weakened variants of *PenotetS*. These variants were created by inserting a GC-rich stem-loop-forming sequence downstream of *PenotetS*. Bases forming the stem are highlighted in red, while those forming the loop are shown in black.

(D) Fluorescence of cells expressing the yellow fluorescent protein mECitrine from each of the *enotetS* series promoters and from the *adh1* promoter in the presence and absence of the inducer anhydrotetracycline (ahTet). Cells were imaged after 24 hours of growth in YES medium in the presence of ahTet or DMSO (solvent control). The images are presented with two different display ranges to enhance the visualization of differences in fluorescence intensities. Scale bar, 10 μm.

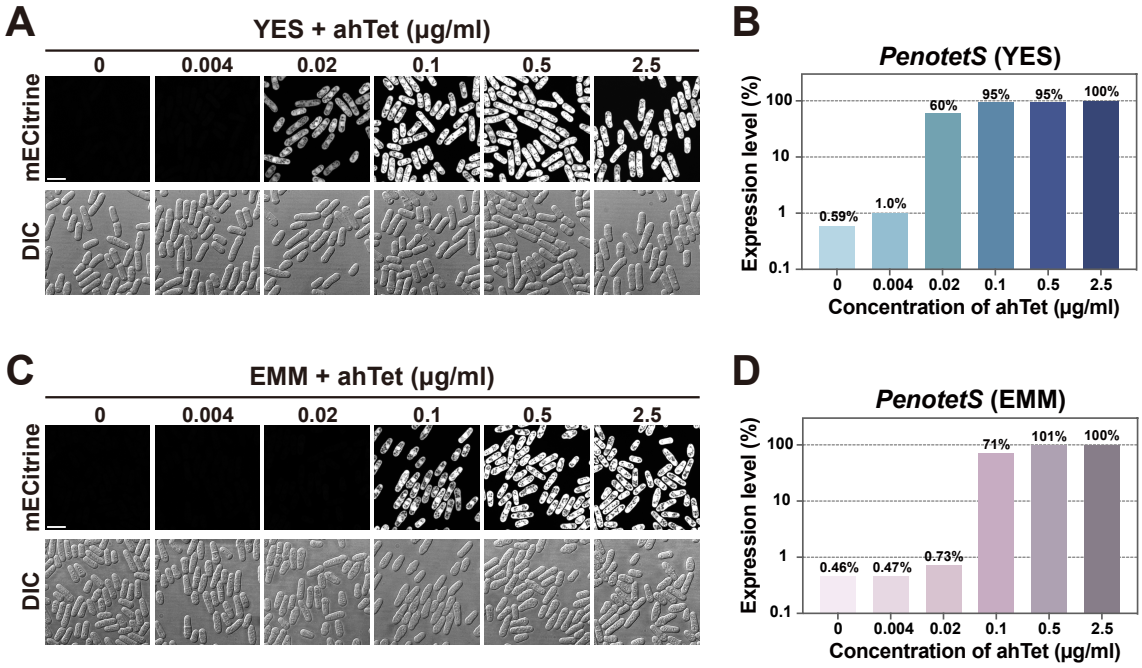

Fig. 2. Inducer dose response of *PenotetS*.

(A) Inducer dose response in YES medium. Cells expressing mECitrine from *PenotetS* were grown in YES medium in the presence of different doses of the inducer ahTet and then imaged. Scale bar, 10 μm.

(B) Quantification of mECitrine fluorescence in the imaging data from the experiment shown in A. The fluorescence level in the presence of 2.5 μg/ml ahTet was used as a reference for normalization (100% expression level).

(C) Inducer dose response in EMM medium. Cells expressing mECitrine from *PenotetS* were grown in EMM medium in the presence of different doses of the inducer ahTet and then imaged. Scale bar, 10 μm.

(D) Quantification of mECitrine fluorescence in the imaging data from the experiment shown in C. The fluorescence level in the presence of 2.5 μg/ml ahTet was used as a reference for normalization (100% expression level).

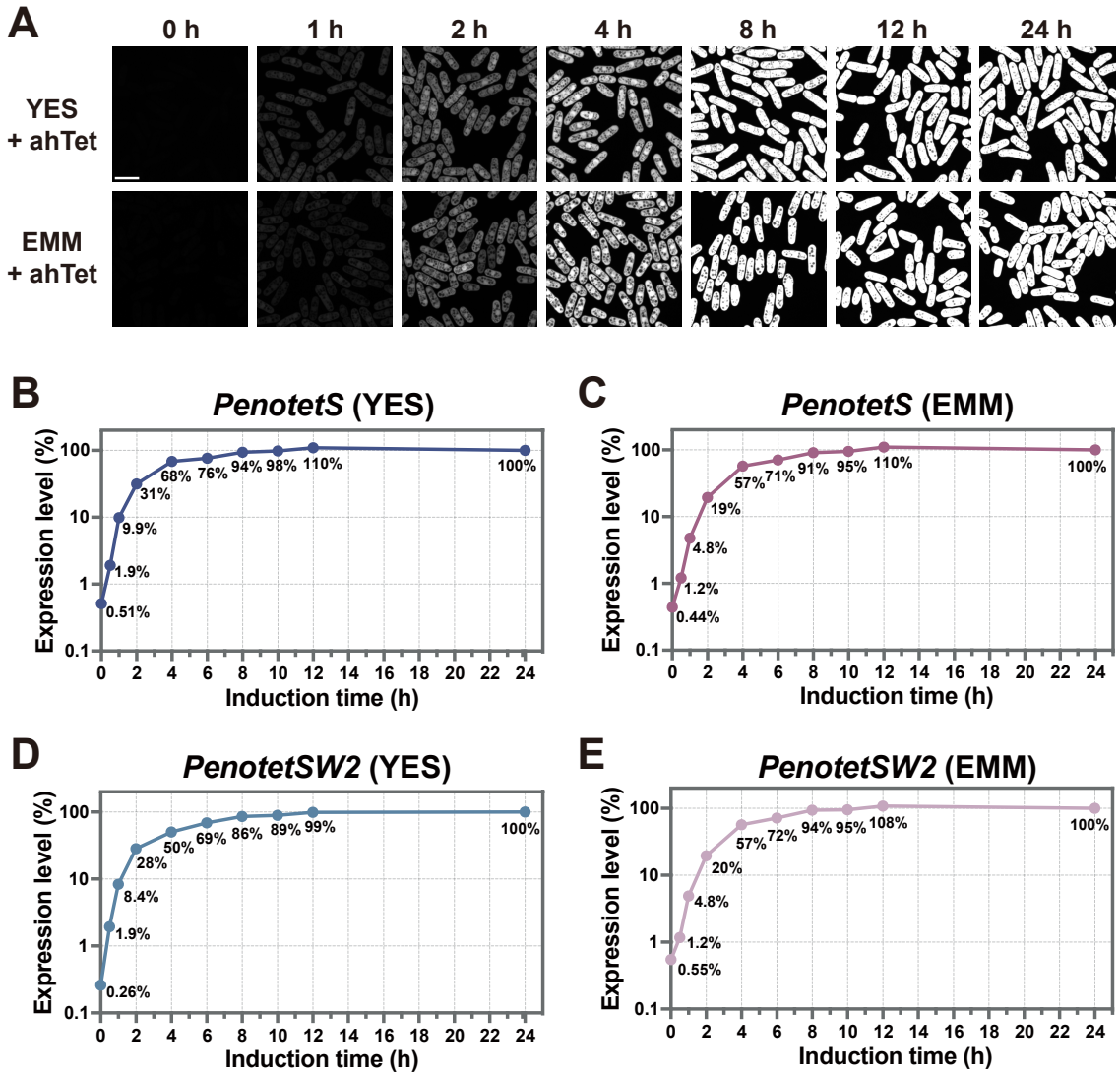

Fig. 3. Induction kinetics of *PenotetS* and *PenotetSW2* in dividing cells.

(A) Time-course analysis of the induction kinetics of *PenotetS* in log-phase cells grown in YES and EMM media. Images of cells expressing mECitrine from *PenotetS* were taken at the indicated time points after the addition of 2.5 μg/ml ahTet to the culture. Scale bar, 10 μm.

(B, C) Quantification of mECitrine fluorescence in the imaging data from the experiment shown in A. The fluorescence level at the 24-hour time point was used as a reference for normalization (100% expression level).

(D, E) Induction kinetics of *PenotetSW2* in log-phase cells grown in YES and EMM media.

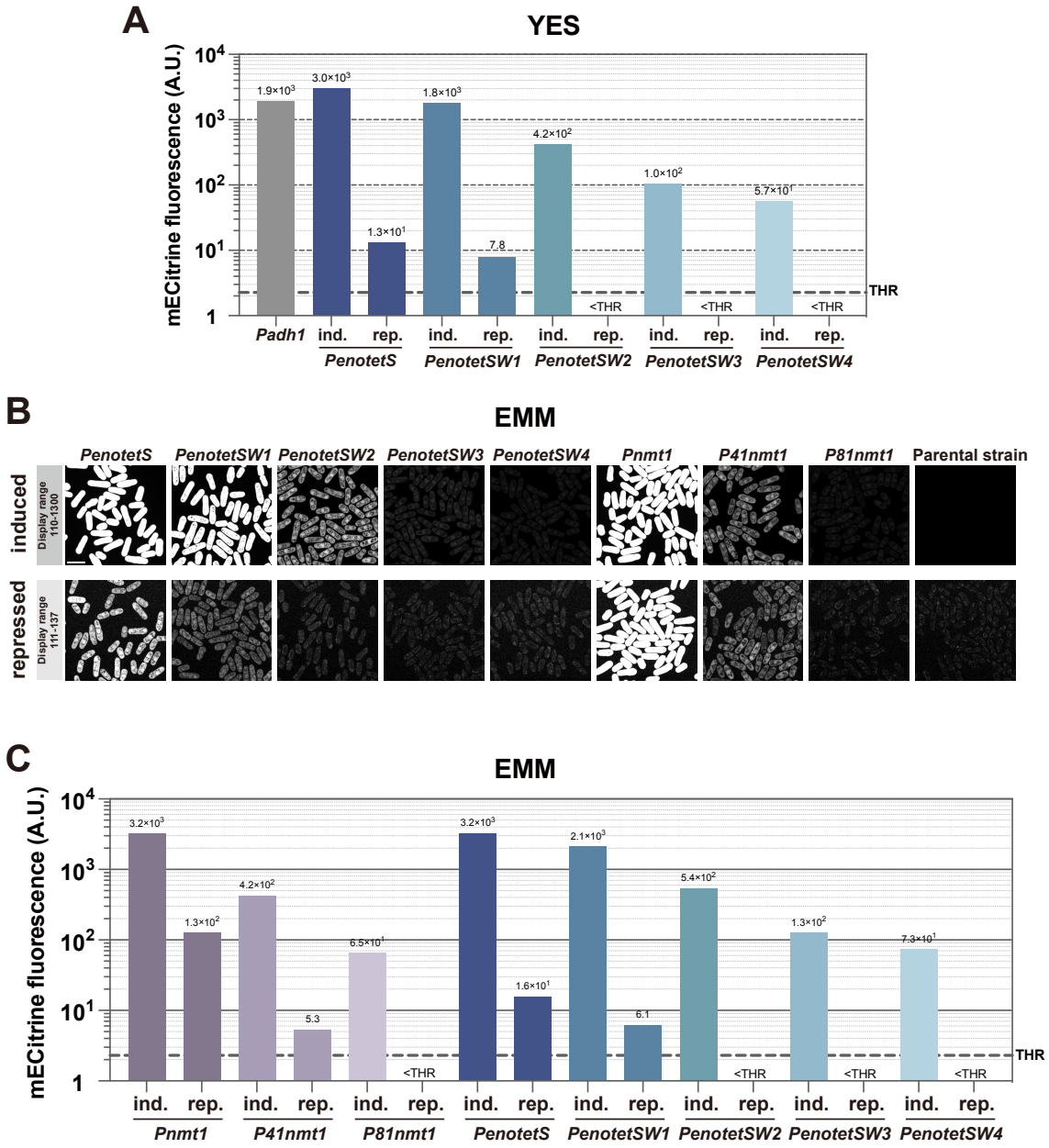

Fig. 4. Expression levels of different promoters.

(A) Expression levels in YES medium. Cells expressing mECitrine from *Padh1* and from each of the *enotetS* series promoters were grown in YES medium under induced conditions (abbreviated as ind., in the presence of ahTet) and repressed conditions (abbreviated as rep., in the absence of ahTet), and then imaged. The quantification

results of the mECitrine fluorescence levels are shown. A thick dashed line represents a threshold (THR) below which the mECitrine fluorescence level cannot be accurately determined. This threshold corresponds to 2% of the average background fluorescence in a parental strain lacking mECitrine.

(B) Expression levels in EMM medium. Cells expressing mECitrine from each of the *enotetS* series promoters were grown in EMM medium under induced conditions (in the presence of ahTet) and repressed conditions (in the absence of ahTet), and then imaged. Cells expressing mECitrine from each of the *nmt1* series promoters were grown in EMM medium under induced conditions (in the absence of thiamine) and repressed conditions (in the presence of thiamine), and then imaged. Scale bar, 10 μm.

(C) Quantification of mECitrine fluorescence in the imaging data from the experiment shown in B.

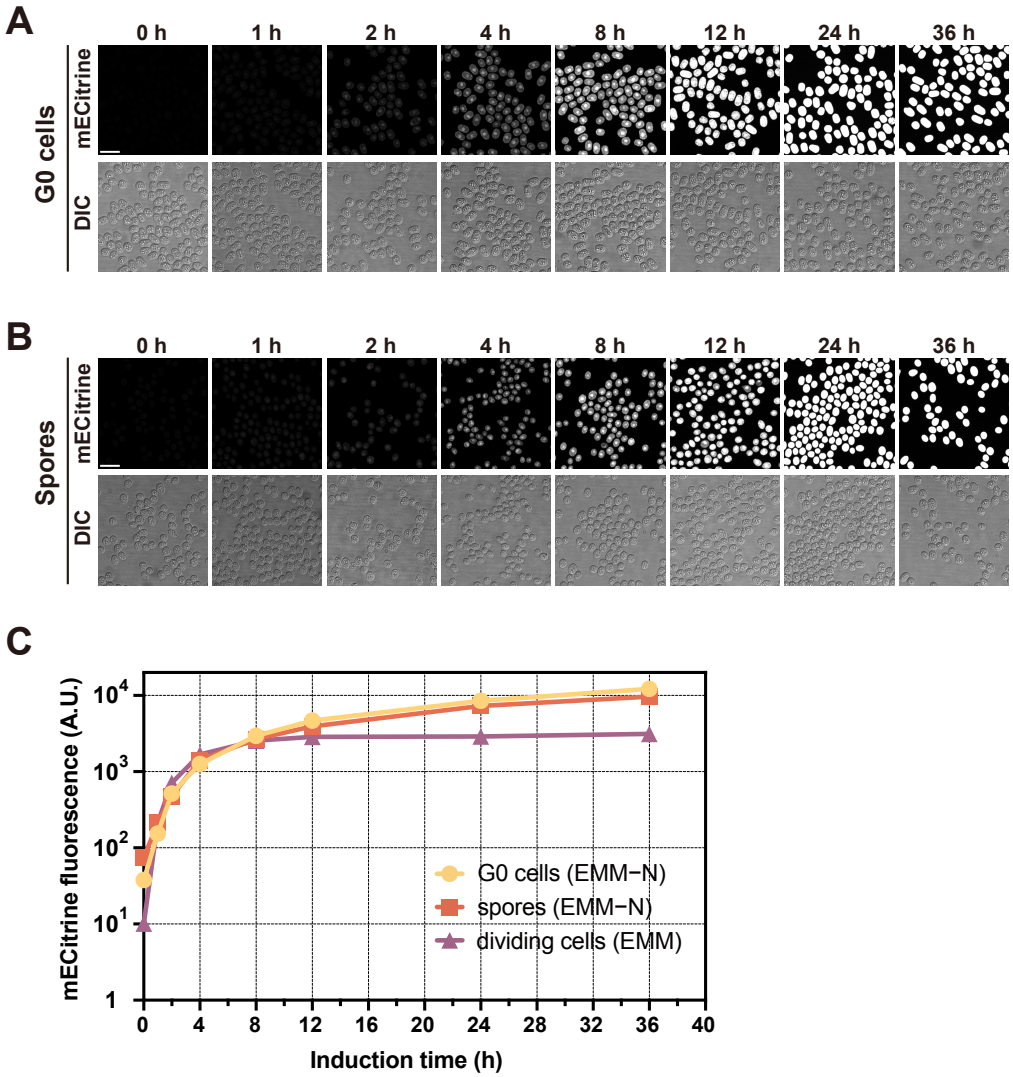

Fig. 5. Induction kinetics of *PenotetS* in quiescent cells.

(A) Time-course analysis of the induction kinetics of *PenotetS* in G0 cells in EMM−N medium. Images were taken at the indicated time points after the addition of 2.5 μg/ml ahTet. Scale bar, 10 μm.

(B) Time-course analysis of the induction kinetics of *PenotetS* in spores in EMM−N medium. Images were taken at the indicated time points after the addition of 2.5 μg/ml ahTet. Scale bar, 10 μm.

(C) Quantification of mECitrine fluorescence in the imaging data from the experiments shown in A and B, as well as a control experiment in which log-phase cells were grown in EMM medium.

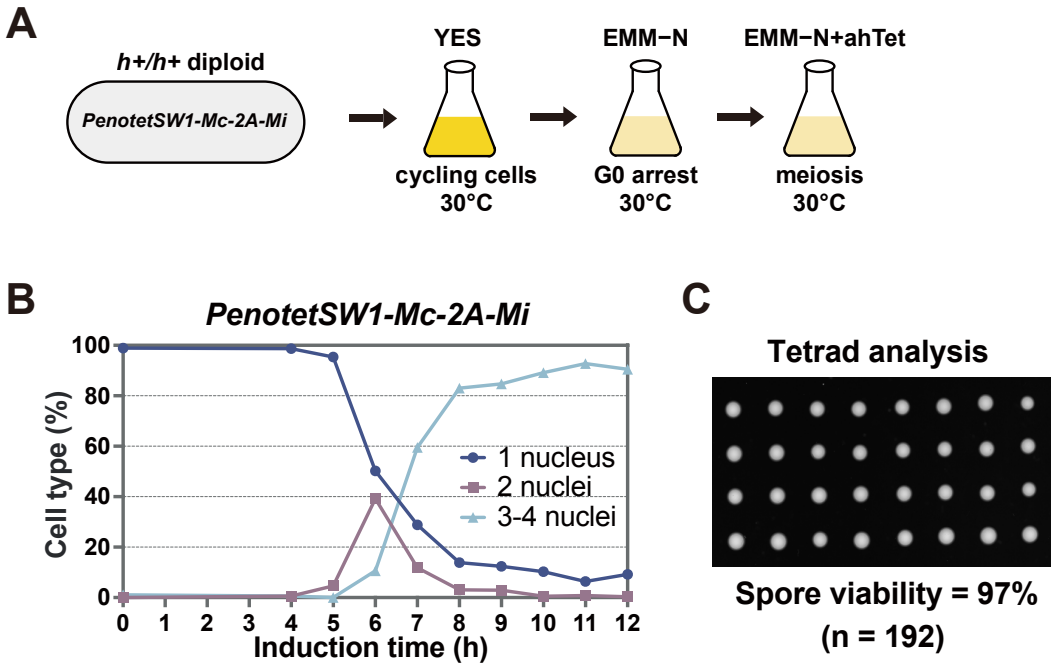

Fig. 6. A new method for synchronous meiosis induction based on the expression of *Mc-2A-Mi* from *PenotetSW1* in *h+/h+* diploids.

(A) Schematic illustrating the new method for synchronous meiosis induction.

(B) Progression of meiosis monitored by DNA staining. Cell samples were stained with the DNA dye SYTOX Green and imaged at the indicated time points after the addition of ahTet. Manual counting was performed to determine the percentages of cells containing different numbers of nuclei.

(C) Viability of spores from induced meiosis. Tetrad analysis was performed on YES plates.

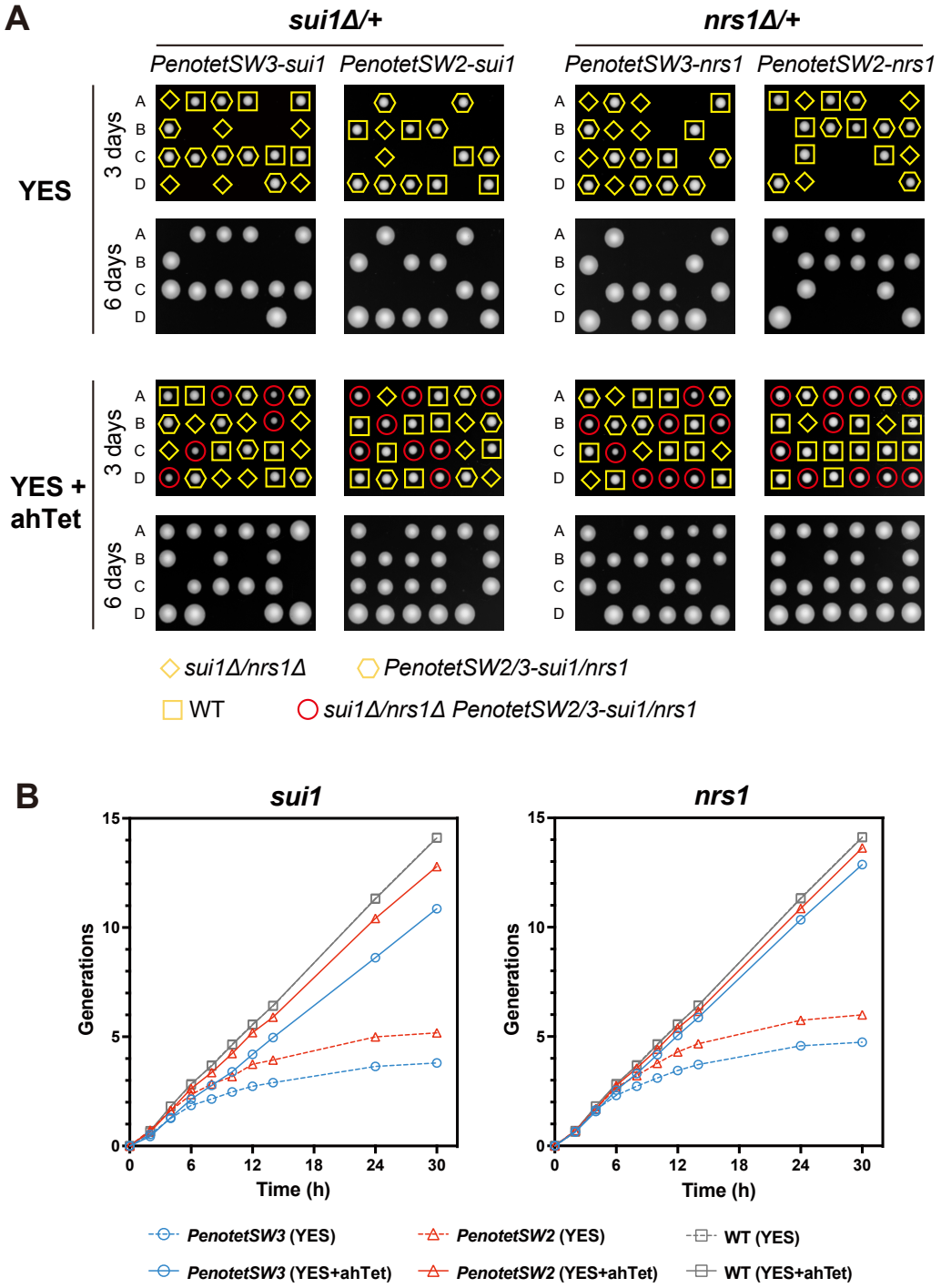

Fig. 7. Generation of conditional loss-of-function mutants using the *enotetS* series promoters.

(A) Tetrad analysis of heterozygous deletion diploids carrying an integration plasmid

expressing the deleted gene from either *PenotetSW2* or *PenotetSW3*. Diploids were sporulated, and the resulting tetrads were dissected on YES plates with and without ahTet. Four spores from a single ascus are labeled A, B, C, and D. The genotype of inviable spores was inferred based on the assumption of 2:2 segregation. Induced expression of *sui1* and *nrs1* rescued the lethality of the respective deletions, while repressed expression did not.

(B) Growth curve analysis showing that the growth defect caused by shutting off gene expression through the removal of ahTet arises rapidly. Cells were initially cultured for 24 hours in YES liquid medium containing ahTet. Following this, cells were washed three times with water and transferred to both ahTet-containing and ahTet-free YES media. The optical density at 600 nm (OD600) of each culture was measured at the indicated time points. Cultures were diluted when the OD600 approached 1.0 to maintain logarithmic growth. The number of generations was calculated based on the OD600 measurements and the dilution ratio.

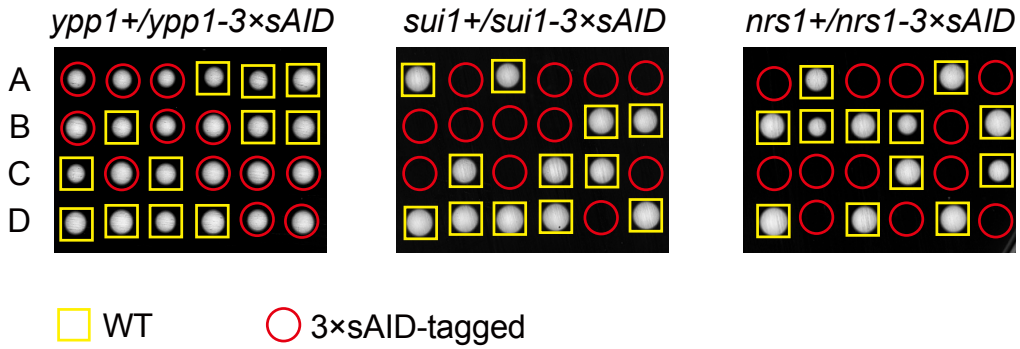

Fig. S1. AID tagging of two essential genes caused lethality.

Tetrad analysis was conducted on heterozygous diploids with one copy of an essential gene endogenously tagged with the 3×sAID tag (Zhang et al., 2022). Diploids were sporulated, and the resulting tetrads were dissected on YES plates.